Zeitschrift: IABSE publications = Mémoires AIPC = IVBH Abhandlungen
Band: 33 (1973)

Artikel: Curved box girder bridges with intermediate diaphragms and supports
Autor: Alam, K.M.A. / Hongladaromp, T. / Lee, S.L.
DOI: https://doi.org/10.5169/seals-25629

Curved Box Girder Bridges with Intermediate Diaphragms and Supports

Ponts courbes en poutres-caissons avec parois intermédiaires et supports

Gekrümmte Kastenträger-Brücken mit Querwänden und Auflagern

K. M. A. ALAM
D. Eng., Research Assistant, Asian Institute of Technology, Bangkok, Thailand

T. HONGLADAROMP
Ph. D., Assistant Professor of Civil Engineering, Asian Institute of Technology, Bangkok, Thailand

S. L. LEE
Ph. D., Professor of Civil Engineering, Asian Institute of Technology, Bangkok, Thailand

Introduction

The use of curved box girder bridges in modern highway systems and interchange facilities has greatly increased. Reviews of the various approximate methods for analyzing such structures can be found in the report of the Subcommittee on Box Girders of the ASCE-AASHO Task Committee on Flexural Members [1] and in the work of McManus, Nasir and Culver [2], in which an extensive list of references is given. Among others, Dabrowski [3, 4], Kuranishi [5], Tung [6], and Konishi and Komatsu [7] suggested approximate methods of analysis. Roll and Aneja [8] conducted an experimental investigation using plastic models of a curved box beam. The orthotropic plate theory with application to multi-cell curved box girders was studied by Yonezawa [9], Ceradini [10], Gavarini [11] and Cheung [12].

Recently, Cheung and Cheung [13] and Meyer and Scordelis [14] treated curved folded plate structures simply supported at the two ends and composed of elements that may in general be segments of conical frustra by finite strip method. Sakai and Okumura [15, 16] modified Vlasov's folded plate theory and applied it to investigate the influence of diaphragms on the behavior of box girders with ribbed plate elements and verified the results experimentally. Chu and Pinjarkar [17] developed a stiffness method for the exact analysis of simply supported curved box girder bridges consisting of horizontal segmental annular decks and vertical cylindrical webs. The stiffness coefficients of the shell elements were based on Hoff's [18] solution of Donnell's equations.

In the present study, the same analytical model used by CHU and PINJARKAR [17] is adopted. The objective is to develope an accurate and efficient method of analysis of the influence of intermediate diaphragms on the behavior of curved box girder bridges simply supported at the ends and subjected to concentrated loads applied at the joints. For the shell elements, Donnell's equations are solved more efficiently with the aid of VLASOV's [19] strain function. The solutions due to unit vertical and radial loads applied at the joints for the case without intermediate diaphragms are obtained and used as influence coefficients to evaluate the effect of intermediate diaphragms under any combination of concentrated live loads applied at the joints. Continuous spans over intermediate supports are also treated in a similar manner.

Fundamental Consideration

Consider a double cell horizontally curved circular box girder bridge, with or without intermediate diaphragms, simply supported at the ends by means of supporting diaphragms, and subjected to unit concentrated loads acting at the joints as shown in Fig. 1. The bridge is assumed to have uniform cross

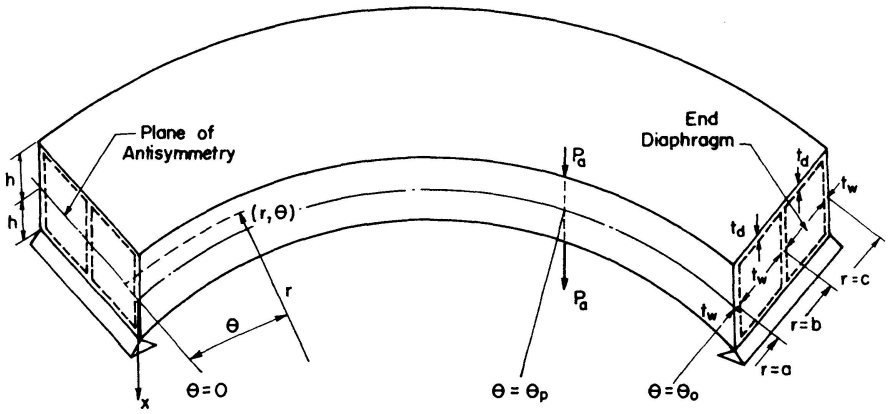

Fig. 1. Simply Supported Curved Box Girder Bridge.

section throughout the span, consisting of the vertical webs which lie on concentric cylindrical surfaces and the horizontal decks which are segmental annular plates. The end diaphragms are assumed to be infinitely rigid in and flexible normal to their planes. It is also assumed that the influence of the in-plane forces on the bending of the plate may be disregarded. This leads to two fourth order partial differential equations which govern the bending and the membrane action of the plate.

A vertical concentrated load acting on a joint of the top deck (Fig. 2a) can be resolved into the symmetrical (Fig. 2b) and antisymmetrical component (Fig. 2c). The solution for the antisymmetrical component will be treated in detail. It will be shown later that, for vertical loads applied at the joints, the

solution for the antisymmetrical component (Fig. 2c) gives practically the same results as the solution for the general loading (Fig. 2a). The slight difference, which is the solution for the symmetrical component (Fig. 2b), is localized and can be obtained by suitable approximation for design purposes. Obviously, it can be readily obtained by a similar analysis as for the antisymmetrical component if an accurate solution is desired.

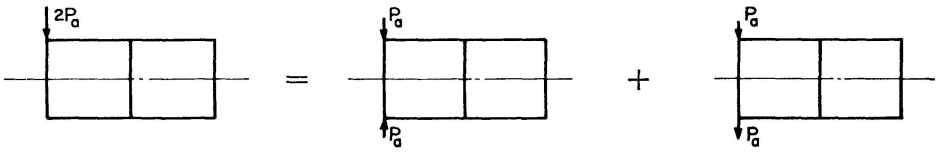

(a) General Loading (b) Symmetrical Loading (c) Antisymmetrical Loading

Fig. 2. Components of Loading.

The cylindrical coordinates (r, θ, x) with origin at the center of curvature and the mid-height of the bridge are indicated in Fig. 1. The radii of curvatures of the inner, the middle and the outer webs with depth $2h$ are denoted by a, b and c respectively. The positions of the end diaphragms are defined by $\theta = 0$ and $\theta = \theta_0$. The positive directions of the displacements and the stress resultants for the segmental annular plate and shell elements are shown in Fig. 3a and b respectively.

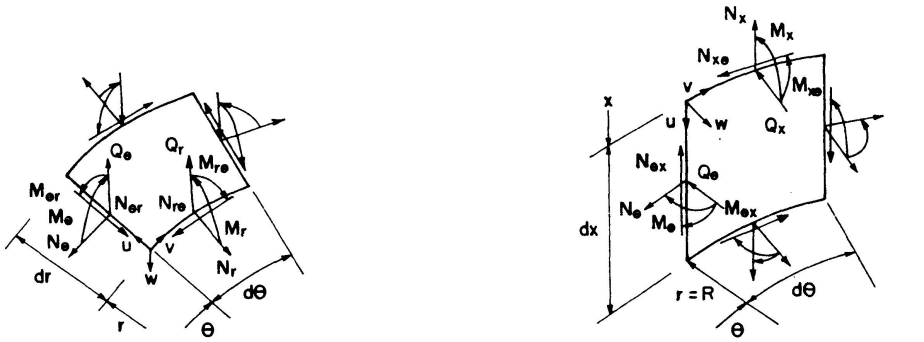

(a) Segmental Annular Plate Element (b) Cylindrical Shell Element

Fig. 3. Positive Directions of Displacements and Stress Resultants.

Segmental Annular Decks in Bending

The homogeneous biharmonic differential equation governing the bending of an elastic annular plate in small deflections [20] is

$$\nabla^4 w = 0, \tag{1}$$

where

$$\nabla^2 = \frac{\partial^2}{\partial \rho^2} + \frac{1}{\rho}\frac{\partial}{\partial \rho} + \frac{1}{\rho^2}\frac{\partial^2}{\partial \theta^2}. \tag{2}$$

In these equations, w is the displacement normal to the plate, positive as shown in Fig. 3a, and $\rho = r/R$ where R is in general the radius of the outer

edge of the annular plate. The general solution of Eq. (1) satisfying the boundary conditions at $\theta=0$ and $\theta=\theta_0$ is obtained in the form, for $k>1$,

$$w = \sum_{m=1}^{\infty} [A_{1m}\rho^k + A_{2m}\rho^{-k} + A_{3m}\rho^{k+2} + A_{4m}\rho^{-k+2}] \sin k\theta, \tag{3}$$

where

$$k = \frac{m\pi}{\theta_0} \tag{4}$$

and A_{1m} to A_{4m} are constants of integration. The expressions for the corresponding stress resultants can be derived from Eq. (3).

Segmental Annular Decks in Plane Stress

The differential equation governing the membrane action of the annular deck plate is [21]

$$\nabla^4 \varphi = 0, \tag{5}$$

where φ is an Airy's stress function. The general solution of Eq. (5) which satisfies the boundary conditions at $\theta=0$ and $\theta=\theta_0$ can be obtained similarly in the form, for $k>1$,

$$\varphi = E t_d R \sum_{m=1}^{\infty} [A_{5m}\rho^k + A_{6m}\rho^{-k} + A_{7m}\rho^{k+2} + A_{8m}\rho^{-k+2}] \sin k\theta, \tag{6}$$

where E is the modulus of elasticity, t_d the thickness of the deck plate and A_{5m} to A_{8m} are the constants of integration. The membrane stress resultants can be readily found and the associated displacement field determined from the stress-displacement relations.

Cylindrical Webs under Curved Edge Loading

The differential equations governing the static behavior of cylindrical shells attributed to Donnell will be adopted [19, 20]. The condition of equilibrium for a cylindrical shell with thickness t_w and radius R are expressed in terms of the displacement components u, v and w (Fig. 3b) by

$$\frac{\partial^2 u}{\partial \zeta^2} + \frac{1-\nu}{2}\frac{\partial^2 u}{\partial \theta^2} + \frac{1+\nu}{2}\frac{\partial^2 v}{\partial \zeta \partial \theta} - \nu\frac{\partial w}{\partial \zeta} = 0, \tag{7a}$$

$$\frac{1+\nu}{2}\frac{\partial^2 u}{\partial \zeta \partial \theta} + \frac{\partial^2 v}{\partial \theta^2} + \frac{1-\nu}{2}\frac{\partial^2 v}{\partial \zeta^2} - \frac{\partial w}{\partial \theta} = 0, \tag{7b}$$

$$\nu\frac{\partial u}{\partial \zeta} + \frac{\partial v}{\partial \theta} - w - \beta^2 \nabla^4 w = 0, \tag{7c}$$

in which ν is the Poisson's ratio and

$$\zeta = \frac{x}{R}, \qquad \beta^2 = \frac{t_w^2}{12R^2}, \qquad \nabla^2 = \frac{\partial^2}{\partial \zeta^2} + \frac{\partial^2}{\partial \theta^2}. \tag{8}$$

Introduce for convenience Vlasov's strain function $\psi(\zeta, \theta)$ which is related to the displacements by

$$u = \frac{\partial^3 \psi}{\partial \zeta \, \partial \theta^2} - \nu \frac{\partial^3 \psi}{\partial \zeta^3}, \tag{9a}$$

$$v = -\frac{\partial^3 \psi}{\partial \theta^3} - (2+\nu) \frac{\partial^3 \psi}{\partial \zeta^2 \, \partial \theta}, \tag{9b}$$

$$w = -\nabla^4 \psi. \tag{9c}$$

It can be readily shown that Eqs. (9) satisfy Eqs. (7) provided

$$\nabla^8 \psi + \frac{1-\nu^2}{\beta^2} \frac{\partial^4 \psi}{\partial \zeta^4} = 0. \tag{10}$$

To satisfy the boundary conditions at $\theta = 0$ and $\theta = \theta_0$ the general solution of Eq. (10) may be assumed in the form

$$\psi = \sum_{m=1}^{\infty} \psi_m(\zeta) \sin k\theta. \tag{11}$$

Substituting Eq. (11) in Eq. (10) leads to

$$\left[\frac{d^2}{d\zeta^2} - k^2\right]^4 \psi_m + 4\lambda^4 \frac{d^4}{d\zeta^4} \psi_m = 0, \tag{12}$$

in which

$$\lambda = \sqrt[4]{\frac{1-\nu^2}{4\beta^2}}. \tag{13}$$

The characteristic equation of Eq. (12) can be shown to be

$$(\alpha_n^2 - k^2)^4 = -4\lambda^4 \alpha_n^4, \tag{14}$$

which can be simplified to a set of four quadratic equations

$$\alpha_n^2 - k^2 = \pm(1 \pm i)\lambda \alpha_n. \tag{15}$$

The eight roots of Eq. (14) are obtained by solving Eq. (15) separately in the form

$$\begin{aligned} \alpha_{1,2} &= \gamma_1 \pm i\beta_1, & \alpha_{3,4} &= -(\gamma_1 \pm i\beta_1), \\ \alpha_{5,8} &= \gamma_2 \pm i\beta_2, & \alpha_{7,8} &= -(\gamma_2 \pm i\beta_2), \end{aligned} \tag{16}$$

where

$$\gamma_{1,2} = \frac{\lambda}{2}\left[\pm 1 + \sqrt{\sqrt{1+k_0^2} + k_0}\right], \qquad \beta_{1,2} = \frac{\lambda}{2}\left[1 \pm \sqrt{\sqrt{1+k_0^2} - k_0}\right], \tag{17}$$

$$k_0 = 2\frac{k^2}{\lambda^2}.$$

Thus the solution of Eq. (12) becomes

$$\psi_m = \sum_{n=1}^{\infty} \bar{B}_{nm} e^{\alpha_n \zeta}, \tag{18}$$

where $\bar{B}_{nm}$ are constants of integration. In view of Eqs. (16), Eq. (18) is expressed in terms of trigonometric and hyperbolic functions and, for loadings

which are antisymmetrical with respect to $x=0$, the terms containing even functions of ζ in the resulting equation are dropped. This leads to

$$\psi = \sum_{m=1}^{\infty} [B_{1m} \cos\beta_1 \zeta \sinh\gamma_1 \zeta + B_{2m} \sin\beta_1 \zeta \cosh\gamma_1 \zeta + B_{3m} \cos\beta_2 \zeta \sinh\gamma_2 \zeta + B_{4m} \sin\beta_2 \zeta \cosh\gamma_2 \zeta] \sin k\theta, \tag{19}$$

in which the arbitrary constants B_{1m} to B_{4m} are linear combination of $\bar{B}_{nm}$. Substituting Eq. (19) in Eqs. (9) yields the displacement components from which the stress resultants can be readily obtained. The details can be found in Ref. [22].

Box Girder Bridge under Unit Loads

The basic problem in the proposed method of analysis is the case of a curved box girder bridge without intermediate diaphragm subjected to antisymmetrical unit loads applied at the joints, as shown in Fig. 2c where $P_a=1$. It will be shown that the effects of loads applied along the joints, as well as the intermediate diaphragm and supports, can be evaluated by means of the linear combination of the individual effect, making use of the influence values obtained from the unit loads solution.

The unit antisymmetrical loads, applied either vertically or radially at the joints with radius R, at $\theta=\theta_p$, is assumed to be uniformly distributed over a small arc of length $2\alpha a$ subtending an angle $2\alpha a/R$ at the center of curvature. These unit vertical or radial loads, $P_R(\theta)$ or $H_R(\theta)$, will be represented by the series

$$P_R(\theta) \text{ or } H_R(\theta) = \sum_{m=1}^{\infty} P_{Rm}(\theta_p) \sin k\theta, \tag{20}$$

where

$$P_{Rm}(\theta_p) = \frac{2}{\theta_0} \int_{\theta_p-\alpha a/R}^{\theta_p+\alpha a/R} \frac{1}{2\alpha a} \sin k\theta \, d\theta = \frac{2}{\theta_0 a} \frac{\sin k\alpha a/R}{k\alpha} \sin k\theta_p \tag{21}$$

and $P_R(\theta)$ is positive in the positive x-direction, while $H_R(\theta)$ is positive if acting in the positive r-direction at the bottom joint (Fig. 4).

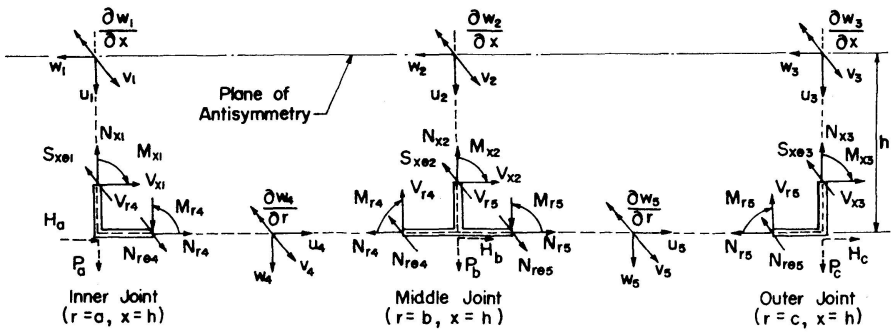

Fig. 4. Positive Directions of Loads, Displacements and Stress Resultants at the Joints.

Boundary Conditions

The general solutions, Eqs. (3), (6) and (19), involve 28 arbitrary constants, viz., A_{1m} to A_{8m} for the inner and outer annular plates, and B_{1m} to B_{4m} for the inner, middle and outer cylindrical shells. These constants are determined from the following 28 boundary conditions. To facilitate the derivation of these equations, the positive directions of the loads, displacements and stress resultants at the joints are shown in Fig. 4. At the inner joint $r=a$ and $x=h$,

$$\begin{aligned}
&(V_{r4})_{\rho=a/b}-(N_{x1})_{\zeta=h/a}+P_a(\theta) = 0, && -(M_{r4})_{\rho=a/b}+(M_{x1})_{\zeta=h/a} = 0,\\
&(N_{r4})_{\rho=a/b}+(V_{x1})_{\zeta=h/a}+H_a(\theta) = 0, && (N_{r\theta 4})_{\rho=a/b}-(S_{x\theta 1})_{\zeta=h/a} = 0,\\
&(w_4)_{\rho=a/b} = (u_1)_{\zeta=h/a}, && \left(\frac{1}{b}\frac{\partial w_4}{\partial \rho}\right)_{\rho=a/b} = \left(\frac{1}{a}\frac{\partial w_1}{\partial \zeta}\right)_{\zeta=h/a},\\
&(u_4)_{\rho=a/b} = -(w_1)_{\zeta=h/a}, && (v_4)_{\rho=a/b} = (v_1)_{\zeta=h/a},
\end{aligned} \tag{22}$$

at the middle joint $r=b$ and $x=h$,

$$\begin{aligned}
&-(V_{r4})_{\rho=1}-(N_{x2})_{\zeta=h/b}+(V_{r5})_{\rho=b/c}+P_b(\theta) = 0,\\
&(M_{r4})_{\rho=1}+(M_{x2})_{\zeta=h/b}-(M_{r5})_{\rho=b/c} = 0,\\
&-(N_{r4})_{\rho=1}+(V_{x2})_{\zeta=h/b}+(N_{r5})_{\rho=b/c}+H_b(\theta) = 0,\\
&-(v_{r\theta 4})_{\rho=1}-(S_{x\theta 2})_{\zeta=h/b}+(N_{r\theta 5})_{\rho=b/c} = 0,\\
&(w_4)_{\rho=1} = (u_2)_{\zeta=h/b} = (w_5)_{\rho=b/c},\\
&\left(\frac{1}{b}\frac{\partial w_4}{\partial \rho}\right)_{\rho=1} = \left(\frac{1}{b}\frac{\partial w_2}{\partial \zeta}\right)_{\zeta=h/b} = \left(\frac{1}{c}\frac{\partial w_5}{\partial \rho}\right)_{\rho=b/c},\\
&(u_4)_{\rho=1} = -(w_2)_{\zeta=h/b} = (u_5)_{\rho=b/c},\\
&(v_4)_{\rho=1} = (v_2)_{\zeta=h/b} = (v_5)_{\rho=b/c}
\end{aligned} \tag{23}$$

and at the outer joint $r=c$ and $x=h$,

$$\begin{aligned}
&-(V_{r5})_{\rho=1}-(N_{x3})_{\zeta=h/c}+P_c(\theta) = 0, && (M_{r5})_{\rho=1}+(M_{x3})_{\zeta=h/c} = 0,\\
&-(N_{r5})_{\rho=1}+(V_{x3})_{\zeta=h/c}+H_c(\theta) = 0, && (N_{r\theta 5})_{\rho=1}+(S_{x\theta 3})_{\zeta=h/c} = 0,\\
&(w_5)_{\rho=1} = (u_3)_{\zeta=h/c}, && \left(\frac{1}{c}\frac{\partial w_5}{\partial \rho}\right)_{\rho=1} = \left(\frac{1}{c}\frac{\partial w_3}{\partial \zeta}\right)_{\zeta=h/c},\\
&(u_5)_{\rho=1} = -(w_3)_{\zeta=h/c}, && (v_5)_{\rho=1} = (v_3)_{\zeta=h/c}.
\end{aligned} \tag{24}$$

In these equations, N_{ri}, $N_{r\theta i}$ and N_{xi} are membrane stress resultants, M_{ri} and M_{xi} the bending stress resultants and $S_{x\theta i}$, V_{ri} and V_{xi} the supplemented shear stress resultants as shown in Fig. 4. The subscripts $i=1, 2$ and 3 are used for the inner, the middle and the outer shell webs respectively, and $i=4$ and 5 for the inner and the outer annular plates respectively. For each set of unit loads, the appropriate $P_R(\theta)$ or $H_R(\theta)$ are retained while the rest are set equal to zero. For instance, for the case shown in Fig. 2c, $P_a(\theta)$ is given by Eq. (20) in view of Eq. (21) with $R=a$.

It is evident that the boundary conditions at the end diaphragms, $(N_{\theta i})_{\theta=0,\theta_0} = (M_{\theta i})_{\theta=0,\theta_0} = (u_i)_{\theta=0,\theta_0} = (w_i)_{\theta=0,\theta_0} = 0$ for $i=1$ to 5, and the boundary conditions on the plane of antisymmetry at mid-depths of the webs, $(N_{xi})_{\zeta=0} = (M_{xi})_{\zeta=0} = (v_i)_{\zeta=0} = (w_i)_{\zeta=0} = 0$ for $i=1, 2$ and 3, are satisfied by the general solutions.

Solution without Intermediate Diaphragm

For six pairs of antisymmetrical unit vertical and radial loads applied simultaneously at the joints $r=a, b$ and c at $\theta=\theta_p$, substituting the appropriate displacement components and stress resultants and the appropriate $P_R(\theta)$ or $H_R(\theta)$ from Eq. (20) into the boundary conditions, Eqs. (22) to (24), leads to a set of 28 simultaneous equations for each harmonic m which can be expressed by

$$[C]\{X\} = \{P\}. \tag{25}$$

In this equation, $[C]$ is a 28×28 coefficient matrix, $\{X\}$ the unknown vector whose elements are the 28 constants of integration and $\{P\}$ the load vector $P_{Rm}(\theta_p)$ given by Eq. (21). The elements of $[C]$, $\{X\}$ and $\{P\}$ are given in Ref. [22]. Finally, Eqs. (25) are solved to obtain the values of $\{X\}=[C]^{-1}\{P\}$ for each pair of antisymmetrical unit loads by setting the others equal to zero. The corresponding displacements and stress resultants at any point (r, θ, x) can be computed by means of the appropriate equations (22).

Treatment of Intermediate Diaphragms and Supports

Unlike the end diaphragms, which are full diaphragms assumed to be rigid in their planes but flexible perpendicular thereto; the intermediate diaphragm is assumed to act as rigid cross bracings in such a way that the diaphragm exerts only concentrated reactions on the joints without introducing resisting moments against joint rotations. In other words, the interactions between the intermediate diaphragm and the double cell box girder consist of pairs of

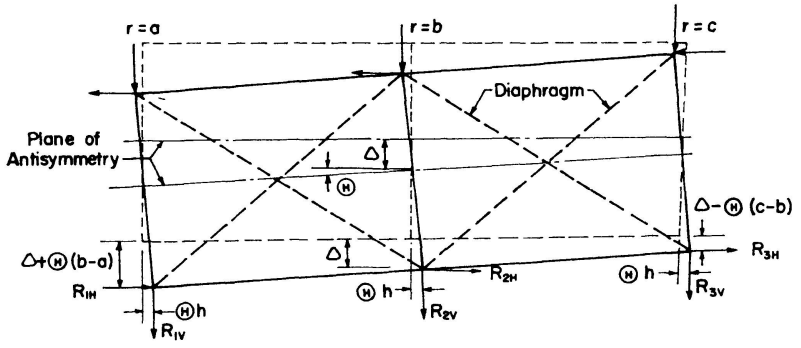

Fig. 5. Rigid Body Displacements and Diaphragm Reactions.

vertical and radial reactive forces at each of the six joints of the cross section (Fig. 5). The reactive forces are assumed to be uniformly distributed over a small arc length along the joint equal to that used in the case of the unit loads. Thus the diaphragm is infinitely rigid in its own plane and, under general loading, it undergoes rigid body displacement, i. e., vertical and radial deflections as well as rotation about the axis of the bridge.

Solution with Intermediate Diaphragm

For antisymmetrical loading, the number of unknown vertical and horizontal diaphragm reactions on the joints reduces from twelve to six, i. e., R_{iV} and R_{iH} for $i=1, 2$ and 3 corresponding to the three bottom joints as shown in Fig. 5. In this case the undetermined rigid body displacement components of the diaphragm reduce from three to two, the vertical deflection Δ of the centroid of the diaphragm and the rotation Θ about this centroidal axis while the radial deflection vanishes. These eight unknowns are determined from the eight equations derived from six compatibility conditions for vertical and radial displacements of the three joints rigidly connected by the diaphragm, and two equilibrium conditions governing the forces acting on the diaphragm. Observe that the equilibrium of forces in the radial direction is identically satisfied by the antisymmetry of forces R_{iH}.

The set of 8 simultaneous equations can be represented in the form

$$\begin{bmatrix} w_{11V} & w_{12V} & w_{13V} & w_{11H} & w_{12H} & w_{13H} & -1 & -(b-a)/h \\ & w_{22V} & w_{23V} & w_{21H} & w_{22H} & w_{23H} & -1 & 0 \\ & & w_{33V} & w_{31H} & w_{32H} & w_{33H} & -1 & (c-b)/h \\ & & & u_{11H} & u_{12H} & u_{13H} & 0 & -1 \\ & & & & u_{22H} & u_{23H} & 0 & -1 \\ & \text{Symmetrical} & & & & u_{33H} & 0 & -1 \\ & & & & & & 0 & 0 \\ & & & & & & & 0 \end{bmatrix}_{\theta=\theta_d} \begin{Bmatrix} R_{1V} \\ R_{2V} \\ R_{3V} \\ R_{1H} \\ R_{2H} \\ R_{3H} \\ \Delta \\ \Theta h \end{Bmatrix} = \begin{Bmatrix} -w_{1jV} \\ -w_{2jV} \\ -w_{3jV} \\ -u_{1jV} \\ -u_{2jV} \\ -u_{3jV} \\ 0 \\ 0 \end{Bmatrix}_{\theta=\theta_p}, \tag{26}$$

in which the influence coefficients w_{ijV} and u_{ijV} are respectively the vertical and radial displacements at the diaphragm at joint i due to unit vertical loads applied at the diaphragm at joint j. The subscript H denotes the corresponding quantities due to unit horizontal loads and the angle θ_d indicates the location of the diaphragm. In the column vector on the right side of Eqs. (26), w_{ijV} and u_{ijV} represent respectively the vertical and horizontal displacements at the diaphragm at joint i due to unit vertical loads applied at joint j along the bridge at $\theta=\theta_p$ (Fig. 1).

The solution of Eqs. (26) yields the reactions as well as the rigid body displacements of the diaphragm at $\theta=\theta_d$ due to unit vertical loads applied at

joint j and $\theta = \theta_p$. The total solution is obtained by the superposition of the effect of the unit vertical loads and those of the diaphragm reactions. Observe that in this linear combination, the influence coefficients are those calculated for the unit vertical and horizontal loads acting on the bridge without diaphragm discussed previously.

Solution with Intermediate Support

The solution for a box girder bridge with intermediate support provided by means of an intermediate diaphragm which in turn is supported by a substructure can be obtained by similar superposition technique with slight modification. In this case, since the rigid body displacement of the diaphragm is arrested by the support, $\Delta = \Theta = 0$ and Eqs. (26) can be used with the deletion of the last two rows and columns.

Numerical Examples and Discussion

Comparison with Results of Finite Strip Analysis

The first example compares the results obtained for a curved box girder bridge without intermediate diaphragms by the finite strip method [13] and those calculated by the proposed method using approximate cross section and loading to preserve symmetry (Fig. 6). The central span length and the mean

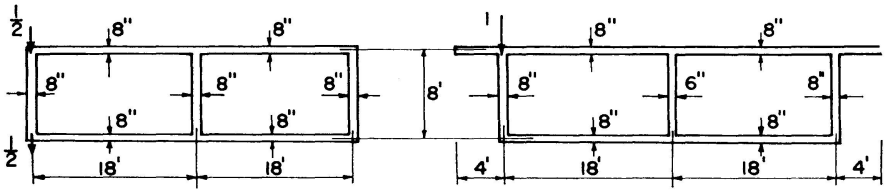

(a) Proposed Method (b) Finite Stip Method (18 Strips)

Fig. 6. Approximate Sections and Loadings.

radius are 100 ft. each with subtended angle of 1 rad. A total of 20 non-zero terms of the series solution, the same as those used in the finite strip analysis, are computed and the results for the stress resultants N_θ and M_r obtained at the midspan for $\nu = 0.16$ are shown in Figs. 7 and 8 for three different radial loading positions, i. e., unit load applied at $\theta_p/\theta_0 = 1/2$ at the inner edge, center and outer edge. The first loading position is illustrated in Fig. 6. The results from both methods of analysis are in good agreement qualitatively in spite of the approximation of the cross section and loading. This agreement holds true also for the longitudinal bending moment M_θ [22]. This verifies that, with the exception of the vicinity of the load, the magnitudes and distribution of

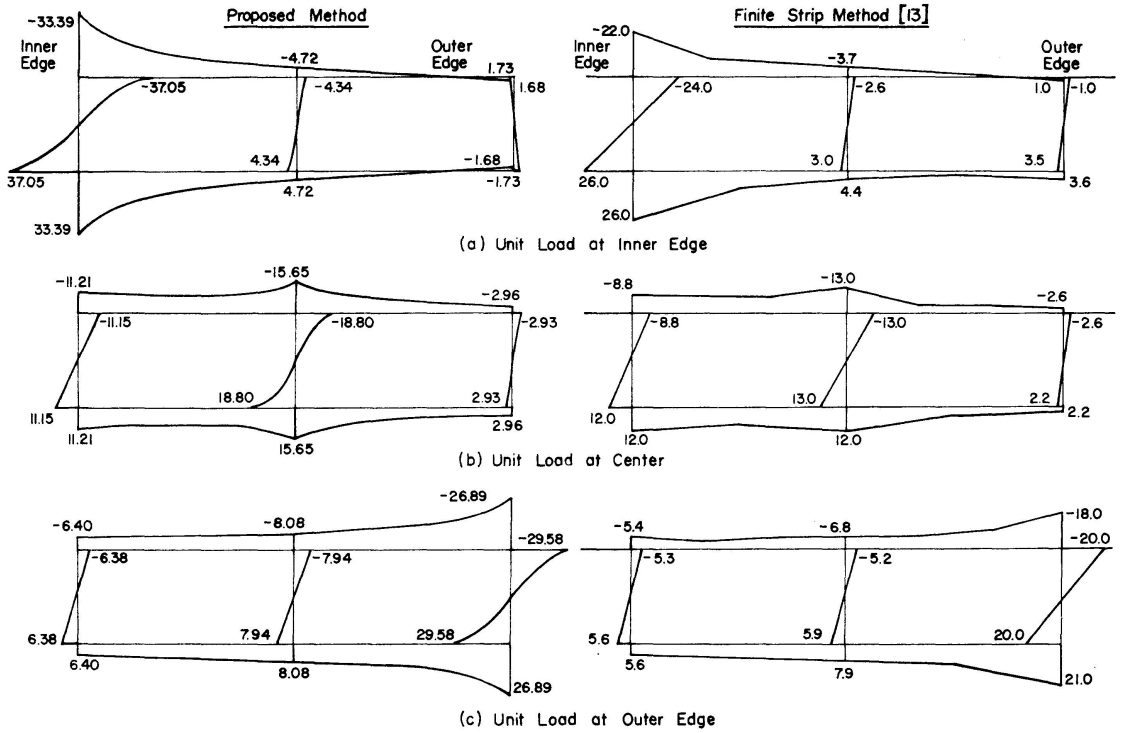

Fig. 7. Comparison of Longitudinal Normal Force $N_\theta \times 10^2$ at Midspan Due to Unit Load at Midspan (Without Diaphragm).

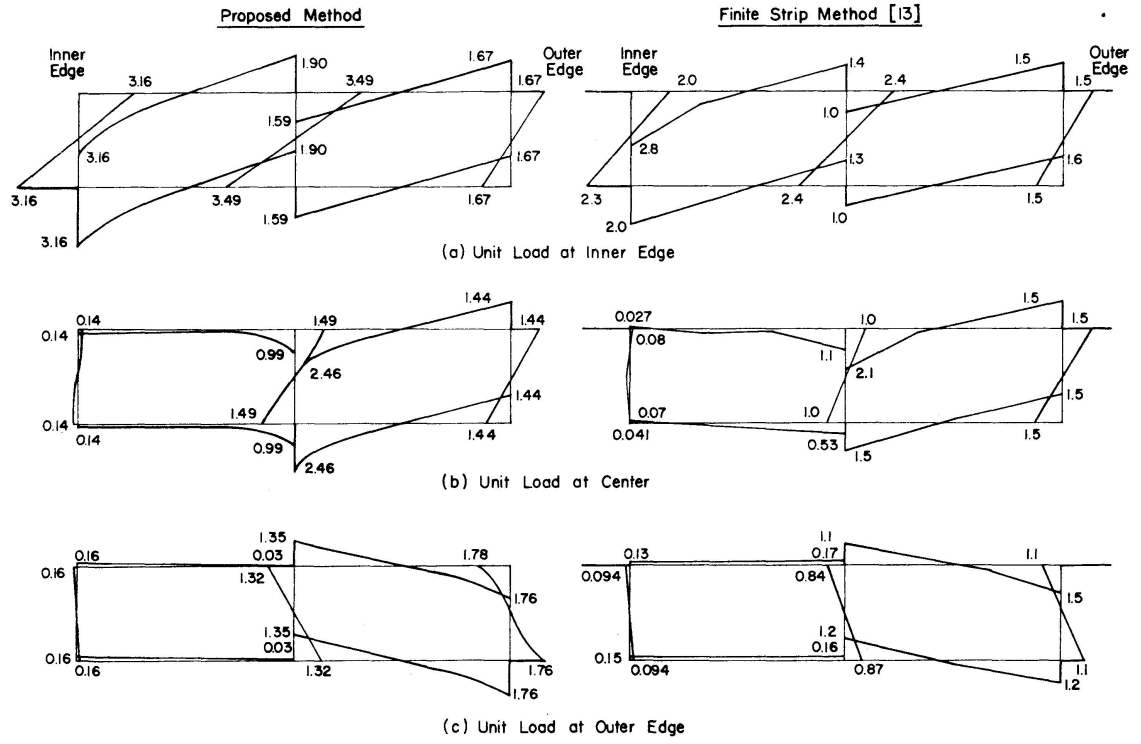

Fig. 8. Comparison of Transverse Bending Moment $M_r \times 10^2$ at Midspan Due to Unit Load at Midspan (Without Diaphragm).

the stress resultants due to the antisymmetrical load component (Fig. 2c) considered in the proposed method are essentially the same as those due to general loading (Fig. 2a).

Influence of Intermediate Diaphragm

The second example deals with curved double cell box girder bridges with or without an intermediate diaphragm. The following set of parameters is chosen for the study: depth to central span ratio = 1/15, depth to total width ratio = 1/3, depth to web thickness ratio = 16, web thickness to deck thickness ratio = 3/4, subtended angle = 1.2 rad. and $\nu = 0.15$. The angle of distribution of the loads or the diaphragm reactions along the inner joint is arbitrarily taken to be 0.005 rad. The series solution is assumed to converge when the amplitude of the current term is less than or equal to $\frac{1}{2}\%$ of the current sum. The results for the displacements and the important stress resultants obtained at quarter sections due to unit vertical loads at $\theta_p/\theta_0 = 1/2$ or 1/4 for different radial loading positions are presented in Figs. 9 to 14 for a comparative study of the influence of the intermediate diaphragm provided at midspan.

It is seen from Figs. 9 and 13a that the cross section of the box girder without the intermediate diaphragm distorts considerably as it deflects under

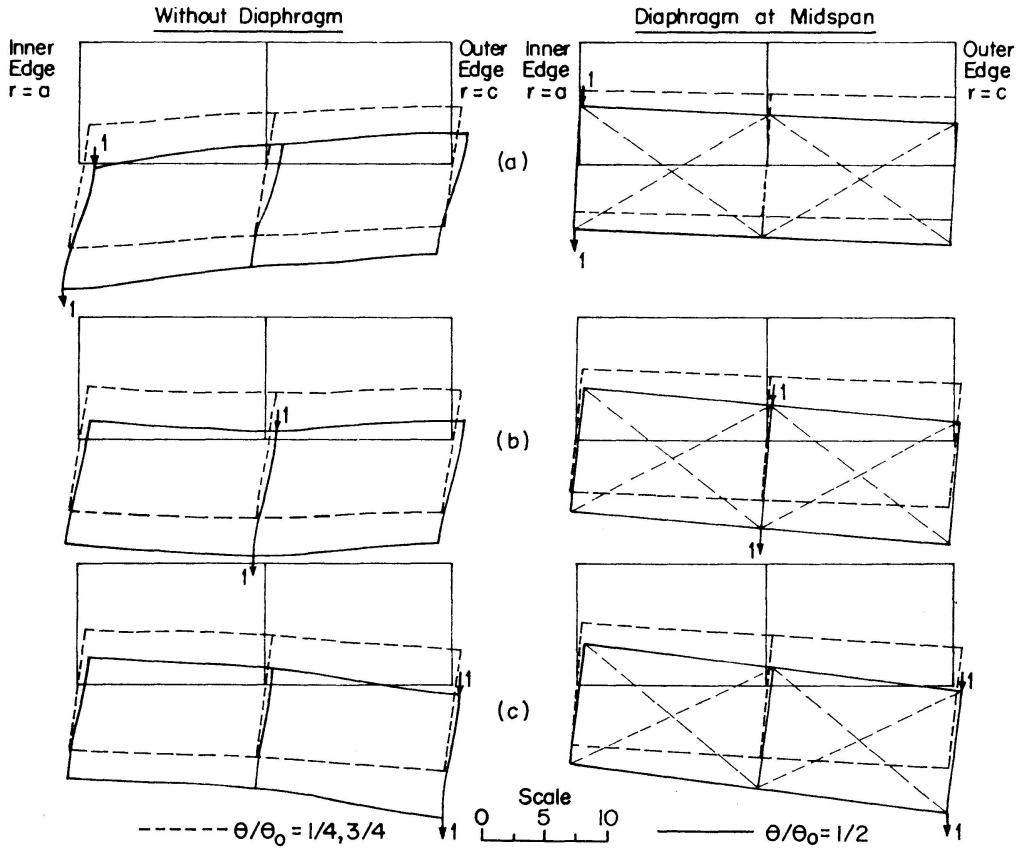

Fig. 9. Deflections (u, w) $(D_d/a^2) \times 10^4$ Due to Unit Loads at Midspan.

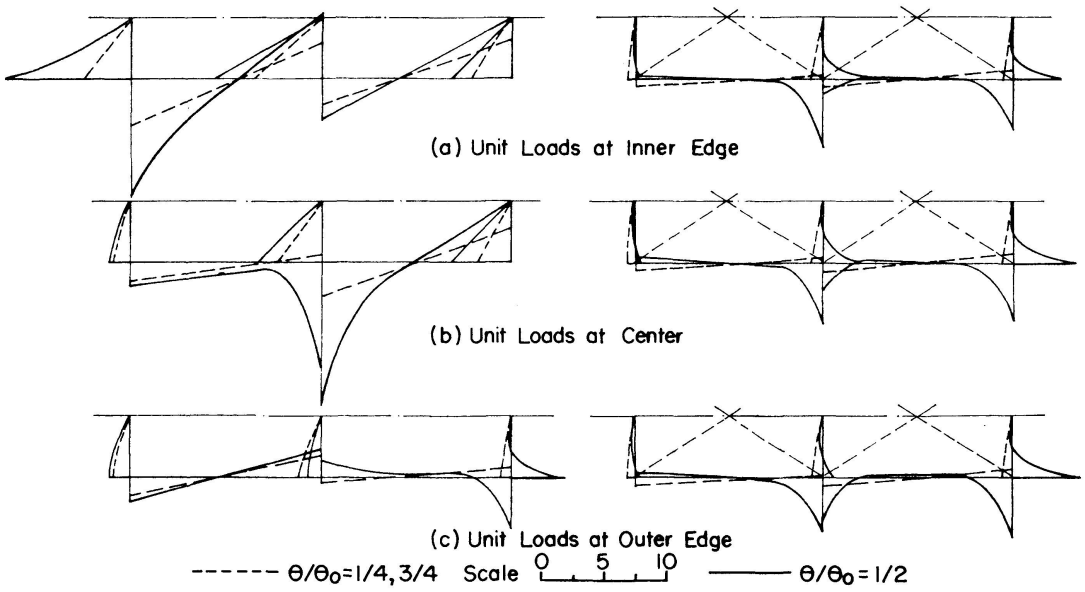

Fig. 10. Transverse Bending Moment $M_r \times 10^2$ Due to Unit Loads at Midspan.

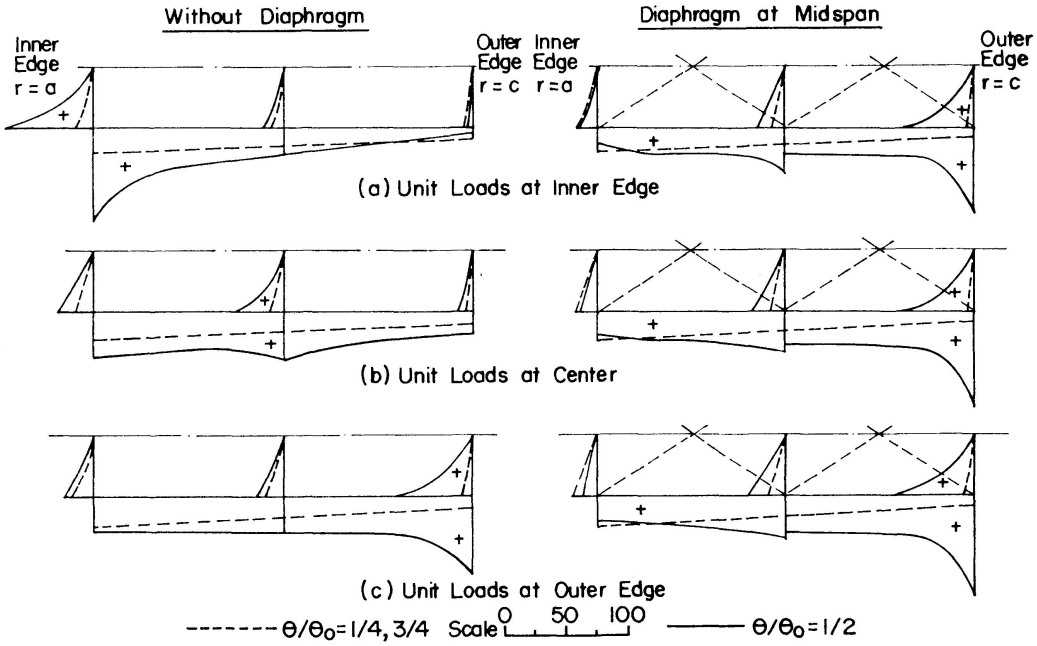

Fig. 11. Longitudinal Normal Force $N_\theta\, a$ Due to Unit Loads at Midspan.

the loads. This distortion, which is maximum under inner edge loadings, causes large transverse bending moments in the cell walls (Fig. 10). For loads acting at the outer joint, the distortion is less prominent because of the greater flexibility of the outer web with longer span length. It is of interest to observe that with the addition of the intermediate diaphragm at midspan, the distortion of the cross section is practically eliminated throughout the span for all cases of joint loadings acting at the midspan. Consequently, the transverse bending moments disappear from the cell walls except locally at the middle

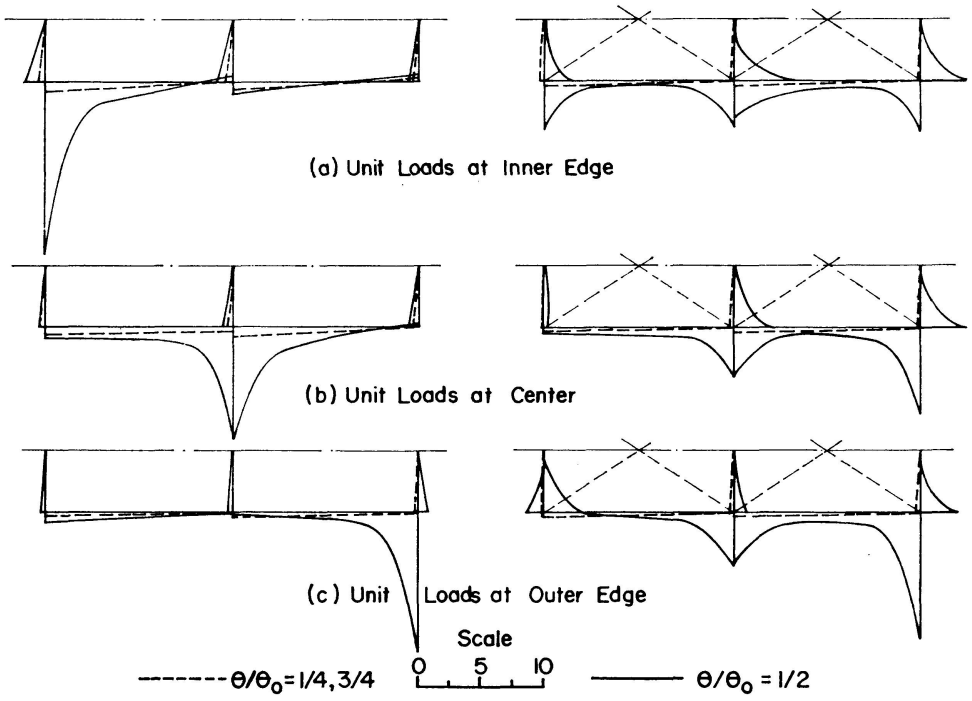

Fig. 12. Longitudinal Bending Moment $M_\theta \times 10^2$ Due to Unit Loads at Midspan.

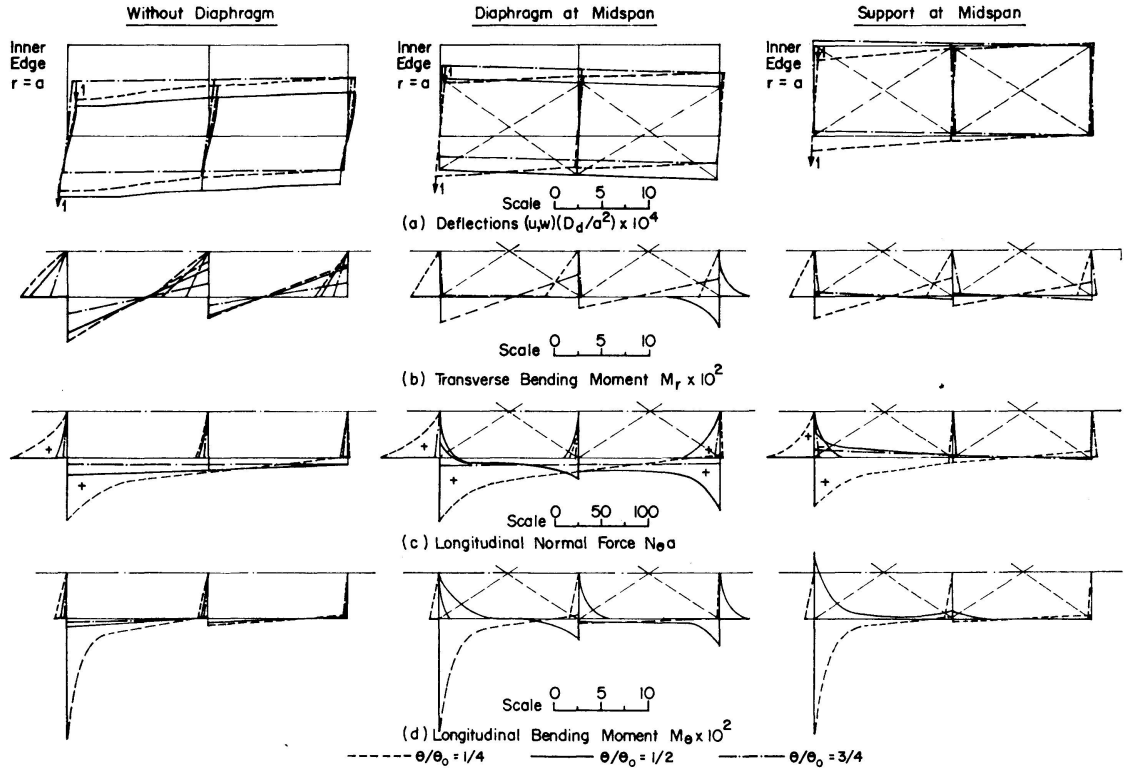

Fig. 13. Displacements and Stress Resultants Due to Unit Loads at Inner Edge at Quarter Span.

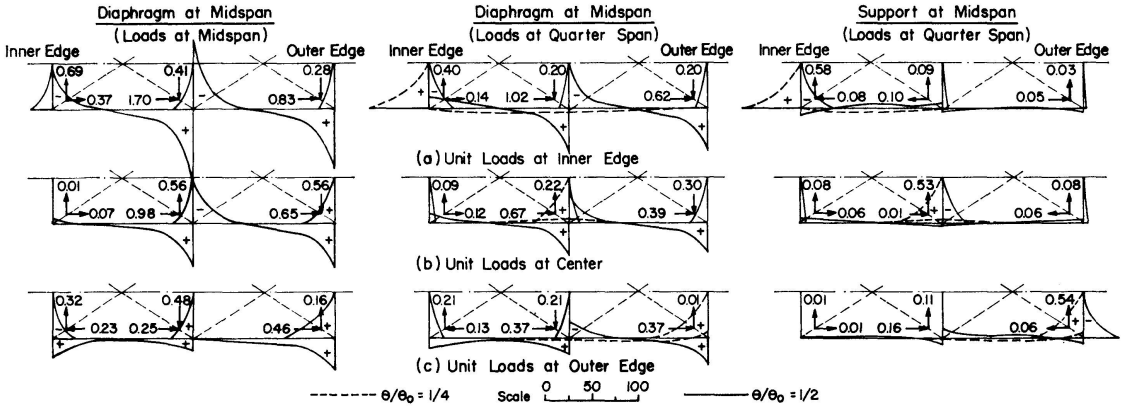

Fig. 14. Transverse Normal Force $N_r\, a$ and Diaphragm Reactions R_{iV} and R_{iH}.

and exterior joints at the diaphragm. However, for loads applied at the quarter span with the diaphragm at the midspan, the distortion and the associated transverse bending moments exist at sections in the vicinity of the loads but with much reduced magnitudes (Figs. 13a and b).

The deflections of the girder decrease considerably with the addition of the intermediate diaphragm which prevents the distortion and increases the overall stiffness of the bridge. The large magnitudes of the displacements which occur under the loads without intermediate diaphragms shift to the outer edge for the addition of the intermediate diaphragm. These behaviors are also repeated with the longitudinal normal forces N_θ in the circumferential direction (Fig. 11). This fact is due to the redistribution of the applied loads by the diaphragm in accordance with the flexibilities of the webs. For sections sufficiently away from the diaphragm, the values N_θ as well as M_θ are hardly influenced by the intermediate diaphragm (Figs. 11, 12, 13c and d). The large magnitudes of M_θ under loads at the midspan reduce significantly with the presence of the diaphragm at that section (Fig. 12).

The concentrated diaphragm reactions cause large transverse normal forces N_r in the neighborhood of the joints (Fig. 14), which are insignificant for the case without intermediate diaphragms except under the loads. However, the values N_r decrease sharply at a small distance from the loads or the reactions.

Continuous Curved Box Girder Bridges

The curved box girder bridge with the same set of parameters investigated in the second example is analyzed for two equal continuous spans over a supported intermediate diaphragm. The results obtained for unit vertical loads applied at the quarterspan are shown in Figs. 13 and 14. The magnitudes of the distortion and the transverse bending moments are significant at sections under the load as expected for the case of a loaded span without intermediate diaphragms. It is interesting to notice that these distortion and transverse bending moment are almost identical to those in the case of a single span

bridge with an intermediate diaphragm at the midspan and subjected to loads at the quarter span (Fig. 13b). This is due to the fact that the intermediate support acts in the same way as the intermediate diaphragm to resist distortions under quarter span loading.

Diaphragm and Support Reactions

The concentrated reactive forces acting on the joints due to the addition of the intermediate diaphragm or support at the midspan are indicated in Fig. 14 for different loading positions. The intermediate diaphragm may be constructed in the form of a truss with chords, verticals and diagonal bracings connected to the bridge at the joints. It should be designed sufficiently stiff to resist the total diaphragm reactions with relatively small displacements in comparison with the distortion of the box sections. Obviously, the severest loading condition for the diaphragm occurs when the loads act on the diaphragm. It is important to note that the diaphragm must resist the total diaphragm reactions without the aid of the box section and that the intermediate support must be designed to resist the total diaphragm reactions.

The supplemented shear stress resultants in the decks and the membrane shear stress resultants in the webs at the end supports due to unit loads at the midspan for the bridge with or without intermediate diaphragm are shown in Fig. 15. The total shears carried by the webs and decks for the middle web loading are respectively 0.986 and 0.014 for the case without intermediate diaphragm, and 0.99 and 0.01 with the intermediate diaphragm. It is interesting to note that the proportions remain practically the same for edge loading in spite of significant changes in shear values of the individual web members.

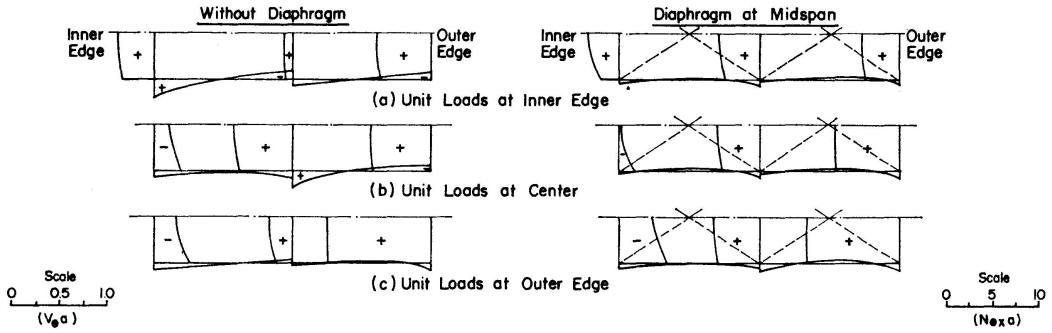

Fig. 15. Supplemented Shear Force $V_\theta\, a$ in Decks and Membrane Shear Force $N_{\theta x}\, a$ in Webs at Supports ($\theta/\theta_0 = 0.1$) Due to Unit Loads at Midspan.

Conclusion

The proposed method of analysis with antisymmetrical joint loads is an accurate and efficient means for analyzing the behavior of curved box girder

bridges with or without intermediate diaphragms and supports. Dealing with the antisymmetrical component of the joint loads greatly simplifies the analysis of the problem and consequently saves computer storage and execution time for its solution. The comparison with the results for the general loadings obtained by the finite strip analysis verifies that the proposed analysis yields practically all the essential details. The effect of the symmetrical load component is local and can be either suitably approximated or readily obtained by a similar analysis if more accurate results are desired.

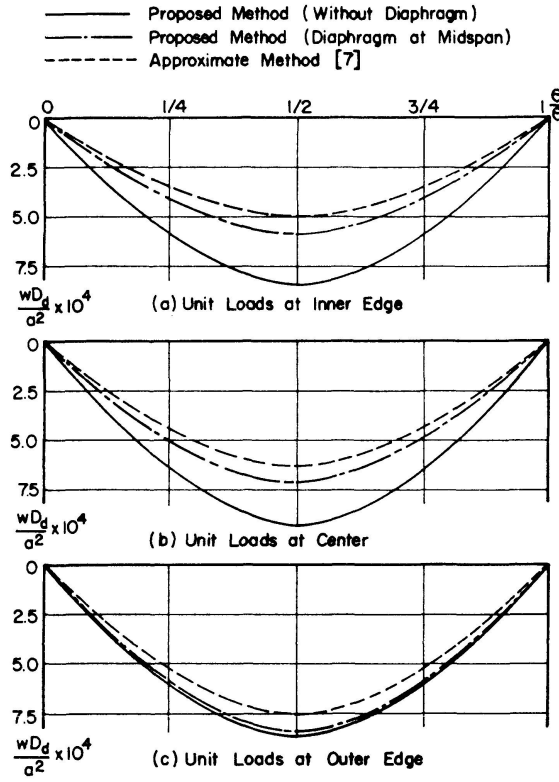

Fig. 16. Comparison of Vertical Deflection along $r=b$ Due to Unit Loads at Midspan.

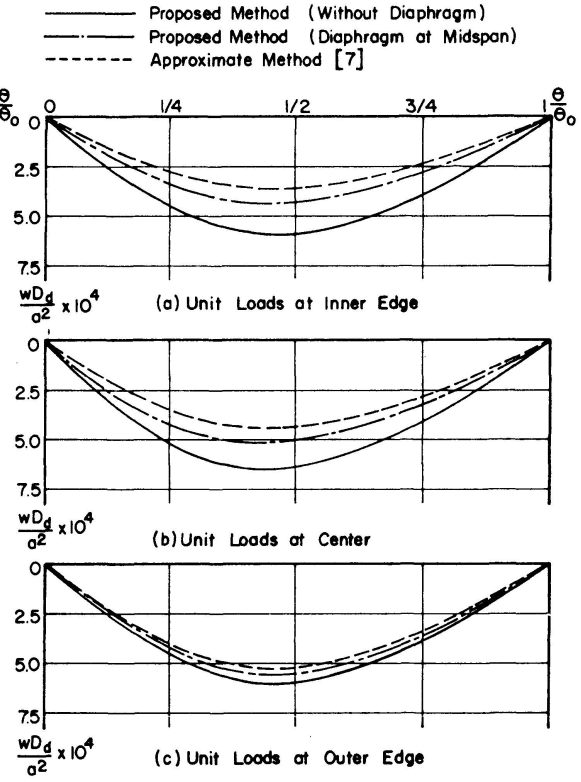

Fig. 17. Comparison of Vertical Deflection along $r=b$ Due to Unit Loads at $\theta_p/\theta_0=1/4$.

It can be seen from Figs. 16 and 17, and the results reported in Refs. [16, 22], that the deflections with intermediate diaphragms tend to approach the approximate solution based on non-deformable cross sections [7]. The latter cannot be applied to the design of curved box girder bridges without intermediate diaphragms. With the provision of an intermediate diaphragm at the midspan, the approximate solutions are in qualitative agreement with the proposed solutions. Better quantitative agreement can be achieved by the use of more intermediate diaphragms.

The use of intermediate diaphragms reduces effectively the cross sectional distortion and the associated transverse bending moments in the cell walls, increases overall stiffness of the bridge, decreases and redistributes the longitudinal normal forces and longitudinal bending moments in the vicinity of the dia-

phragm sections. The general conclusions with regard to the response of curved box girder bridges with or without intermediate diaphragms predicted by the proposed method agree well with the experimental observations reported in Ref. [16].

The proposed method of analysis can be extended without fundamental difficulties to analyze the behavior of curved steel box girder bridges with rib-stiffened decks. In this case the equations governing the bending and membrane action of the deck plates, which are assumed to be isotropic in this study, are to be replaced by appropriate equations which take the orthotropy into account.

References

1. The Subcommittee on Box Girders of the ASCE-AASHO Task Committee on Flexural Members: Progress Report on Steel Box Girder Bridges. J. Struc. Div., ASCE, Vol. 97, No. ST 4, Proc. Paper 8068, p. 1175–1185, April 1971.
2. McManus, P. F., Nasir, G. A. and Culver, C. G.: Horizontally Curved Girders – State of The Art. J. Struc. Div., ASCE, Vol. 95, No. ST 5, Proc. Paper 6546, p. 853–870, May 1969.
3. Dabrowski, R.: Näherungsberechnung der gekrümmten Kastenträger mit verformbarem Querschnitt. (Approximate Calculation of Curved Box Girders with Deformable Cross Section.) Preliminary Pub., IABSE, 7th Congress, 1964.
4. Dabrowski, R.: Wölbkrafttorsion von gekrümmten Kastenträgern mit nichtverformbarem Profil. (Warping Torsion of Curved Box Girders With Non-deformable Profile.) Stahlbau, Vol. 34, No. 5, p. 135–141, May 1965.
5. Kuranishi, S.: Analysis of Thin-Walled Curved Beams. Trans., JSCE, No. 108, p. 7–12, August 1964.
6. Tung, D. H. H.: Analysis of Curved Twin Box Girder Bridges. ASCE Struc. Eng. Conference, Seattle, May 8–12, 1967.
7. Konishi, I. and Komatsu, S.: Three Dimensional Analysis of Curved Girder with Thin-walled Cross Section. Pub., IABSE, p. 143–204, 1965.
8. Roll, F. and Aneja, I.: Model Tests of Box Beam Highway Bridges with Cantilevered Deck Slabs. ASCE Transportation Eng. Conference, Phil., Pa., October 17–21, 1966.
9. Yonezawa, H.: Moments and Free Vibrations in Curved Girder Bridges. J. Eng. Mech. Div., ASCE, Vol. 88, No. EM 1, Proc. Paper 3052, p. 1–21, Feb. 1962.
10. Ceradini, G.: Theorie des Ponts Courbes a Poutres Multiples. (Theory of Multi-Girder Curved Bridges), Pub., IABSE, p. 51–63, 1965.
11. Gavarini, C.: Theoria dei Ponti in Curva a Travi Multiple. (Theory of Multi-Girder Curved Bridges), Construzioni metalliche, No. 3, p. 219, 1965.
12. Cheung, Y. K.: The Analysis of Cylindrical Orthotropic Curved Bridge Decks. Pub., IABSE, Vol. 29-II, Dec. 1969.
13. Cheung, M. S. and Cheung, Y. K.: Analysis of Curved Box Girder Bridges by Finite Strip Method. Pub., IABSE, Vol. 31-I, p. 1–19, 1971.
14. Meyer, C. and Scordelis, A. C.: Analysis of Curved Folded Plate Structures. J. Struc. Div., ASCE, Vol. 97, No. ST 10, Proc. Paper 8434, p. 2459–2480, Oct. 1971.
15. Okumura, T. and Sakai, F.: The Cross Sectional Deformation of Box-Girders and the Influence of Intermediate Diaphragms. Trans. JSCE, Vol. 2, Part 1, 1971.

16. Sakai, F. and Okumura, T.: Influence of Diaphragms on Behavior of Box Girders with Deformable Cross Section. Preprint, IABSE 9th Congress, Amsterdam, May 1972.
17. Chu, K. H. and Pinjarkar, S. G.: Analysis of Horizontally Curved Box Girder Bridges. J. Struc. Div., ASCE, Vol. 97, No. ST 10, Proc. Paper 8453, p. 2481–2501, October 1971.
18. Hoff, N. J.: Boundary Value Problems of the Thin-walled Circular Cylinder. J. Appl. Mech., p. 343–350, December 1954.
19. Vlasov, V. Z.: Allgemeine Schlentheorie und ihre Anwendung in der Technik. Akademie-Verlag, Berlin, 1958.
20. Timoshenko, S. P. and Woinowsky-Krieger, S.: Theory of Plates and Shells. 2nd Ed., McGraw-Hill Co., N. Y., 1959.
21. Timoshenko, S. P. and Goodier, J. N.: Theory of Elasticity. 3rd Ed., McGraw-Hill Co., N. Y., 1970.
22. Alam, K. M. A.: Curved Box Girder Bridges with Intermediate Diaphragms and Supports. D. Eng. Dissertation, Asian Institute of Technology, Bangkok, Aug. 1972.

Summary

The static behavior of simply supported curved box girder bridges with or without intermediate diaphragms subjected to concentrated joint loads is investigated. The analytical model consists of a double cell box section with horizontal annular segmental deck plates and vertical cylindrical shell webs. The solutions due to unit antisymmetrical vertical and radial loads applied at the joints for the case without intermediate diaphragms are obtained and used as influence coefficients to evaluate the effect of intermediate diaphragms under vertical loads applied at the joints. Continuous spans over intermediate supports are treated in a similar manner. Numerical examples are presented and the influence of intermediate diaphragms is discussed.

Résumé

On étudie le comportement statique de poutres de ponts en caisson simplement supportées, avec ou sans panneaux sous l'influence de charges concentrées. Le modèle analytique est constitué d'une section de caisson à doubles cellules avec des couvre-joints horizontaux annulaires et par des plaques verticales cylindriques. On obtient les solutions dues aux charges antimétriques verticales et radiales appliquées aux joints dans le cas sans panneaux et on s'en sert de coefficients d'influence pour évaluer l'effet de panneaux sous des charges verticales agissant aux joints. Des ouvertures continues sur des supports intermédiaires sont traitées de façon analogue. On donne des exemples numériques et on discute de l'influence des panneaux.

Zusammenfassung

Es wird das statische Verhalten einfach unterstützter gekrümmter Kastenträgerbrücken mit oder ohne Querwände unter Einwirkung konzentrierter Belastungen untersucht. Das analytische Modell besteht aus einem doppelzelligen Kastenquerschnitt mit horizontalen ringförmigen Segmentdeckplatten und vertikalen zylindrischen Scheiben. Man erhält die Lösungen infolge antimetrischer vertikaler und radialer Belastungen an den Verbindungen für den Fall ohne Querwände und benützt sie als Einflusskoeffizienten, um die Wirkung von Querwänden unter vertikalen an den Verbindungen wirkender Lasten abzuschätzen. Durchlaufende Öffnungen über Zwischenstützen werden in analoger Weise behandelt. Es werden Zahlenbeispiele gegeben und der Einfluss von Querwänden diskutiert.